J Mater Sci (2011) 46:1351–1358
DOI 10.1007/s10853-010-4926-1

Oxidation behavior and effect of oxidation on tensile properties of Ti60 alloy

Weiju Jia · Weidong Zeng · Xuemin Zhang · Yigang Zhou · Jianrong Liu · Qingjiang Wang

Received: 22 June 2010 / Accepted: 14 September 2010 / Published online: 28 September 2010

Abstract Oxidation behavior of a near-alpha Ti60 titanium alloy was investigated in the temperature range of 600–750 °C for up to 100 h exposure. The results showed that the oxidation kinetics of Ti60 alloy followed parabolic kinetics below 700 °C but parabolic-linear kinetics above 700 °C. The total activation energy was calculated to be 256 kJ/mol over the whole temperature range. The oxidation products were TiO_2 after thermal exposure at 700 °C for 100 h, but a mixture of TiO_2 and a small amount of Al_2O_3 for the specimens oxidized at 750 °C for 50 h. The grain boundaries were preferred sites for oxidation products formation during the oxidation. The tensile tests were performed at room temperature for specimens before and after oxidation. Both of the strength and ductility decreased for the specimens with oxide scale. However, both of them increased when the oxide scale was removed before testing.

Introduction

Titanium alloys have been considered as a candidate material for fabrication of components to be used in the compressor section of aerospace engines due to their superior strength–weight ratio and corrosion resistance. However, the high-temperature oxidation resistance of Ti-based alloy is rather poor, which limits the highest operating temperature of titanium alloys under 600 °C [1, 2]. Thus, how to improve its high-temperature oxidation resistance has become an attracting research field.

Improvement of oxidation resistance including minimized embrittlement of Ti-based alloys can essentially be achieved by addition of certain elements to the alloy, surface modification techniques, and protective coatings [3–6]. Numerous attempts have been made to provide improved oxidation resistance by protective coating, however, as far as is known from the literature, oxidation-resistant coatings have not yet been brought into real service [7]. Near-alpha titanium alloys developed by addition of alpha stabilizing elements have made it possible to increase the service temperature up to 600 °C, so called "high-temperature titanium alloy". The typical high-temperature titanium alloys are IMI834 and Ti-1100 alloy [8, 9], which have good creep resistance against high temperature and excellent mechanical properties at the servicing temperatures of 600 °C. Ti60 alloy is a near-alpha high-temperature titanium alloy developed by Institute of Metal Research in China. It belongs to Ti–Al–Sn–Zr–Mo–Si series titanium alloy, which is similar to IMI834 alloy. Compared with the alloy IMI834, Ti60 alloy also possesses excellent creep resistance and mechanical properties at high temperatures, and it is considered for 600 °C applications, such as for the manufacture of the disc in aero-engine [10].

Like other titanium alloys, Ti60 alloy readily absorbs oxygen and leads to oxidation when used at elevated temperatures, particularly above 500 °C in air. Interaction of titanium alloys with oxygen causes not only loss of material by formation of oxides, but also embrittlement in the subsurface zone of the component due to oxygen enrichment, generally known as "alpha-case". This brittle alpha-case severely affects the mechanical properties of the

W. Jia · W. Zeng (✉) · X. Zhang · Y. Zhou
State Key Laboratory of Solidification Processing, School of Materials, Northwestern Polytechnical University, Xi'an 710072, China
e-mail: zengwd@nwpu.edu.cn

J. Liu · Q. Wang
Institute of Metal Research, Chinese Academy of Sciences, Shenyang 110016, China

alloys and limits their utilization [11, 12]. Several investigations have been performed to characterize the oxidation behavior of IMI834 and Ti-1100 alloy at the temperature range of 600–800 °C [13, 14]. For Ti60 alloy, the oxidation kinetics above 620 °C has been studied [15, 16]. However, at the region of temperature 600–750 °C, little information is available on the kinetic and the high-temperature oxidation mechanisms of Ti60 alloy. Moreover, there is no report on the detailed investigation of alpha-case formation and its effect on the tensile properties of Ti60 alloy.

In this paper, the oxidation behavior of Ti60 alloy, including oxidation kinetics, oxidation mechanisms, and oxide scale formation are studied. Additionally, an oxidation model is proposed for the alpha-case formation to predict the extent of oxidation during the high temperatures. The room temperature tensile properties of specimens before and after oxidized are also investigated.

Experimental

The material used in this study was Ti60 alloy rod with the diameter of 120 mm. Its chemical composition (mass%) was Ti–5.8Al–4.0Sn–3.5Zr–0.4Mo–0.4Nb–1.0Ta–0.4Si–0.06C. The beta transus for this alloy is approximately 1050 °C. The alloy was solution treated at 1015 °C for 2 h, oil cooled and then aged at 700 °C for 2 h, air cooled. The initial microstructure of Ti60 alloy composed by approximately 40% equiaxed primary α and fine transformed β matrix is shown in Fig. 1. The distribution of the primary α phase is relatively homogeneous and the transformed β consists of α platelets with thin layer of β phase retained between them.

Oxidation tests of the specimens with dimensions of $\varnothing$ 10 mm × 8.8 mm were conducted at 600–750 °C in static air. The specimens placed in alumina crucibles were oxidized at desired temperatures and then air cooled to room temperature. The weight of specimens before and after oxidation were measured using an analytic balance (AL204) providing an accuracy of 0.0001 g to characterize the oxidation kinetics. Subsequent to oxidation, the surface and cross-sectional morphologies of the specimens were analyzed using optical and scanning electron microscopy (SUPRATM55). Phase identifications of Ti60 alloy after oxidation were performed by X' Pert PRO X-ray Diffractometer with Cu Ka radiation. Additionally, the depth of the oxide scale was measured from the cross-sections of the specimens by utilizing HXP-1000TM microhardness tester.

Room temperature tensile test were conducted to determine the tensile properties of the alloy before and following thermal exposure at 600, 700, and 750 °C for 100 h. In order to investigate the effect of oxide scale on the tensile properties of Ti60 alloy, specimens having the oxide scale removed also prepared for tensile tests.

Results and discussion

Oxidation behavior

Figure 2 presents the variation of weight gain data with respect to oxidation time. As can be seen, the weight gain increases with increasing time and temperature, as expected. It is clear that the oxidation resistance of Ti60 alloy is good at 600 °C but it degrades when the temperature rise to 650 °C and above. All of the curves exhibit similar feature

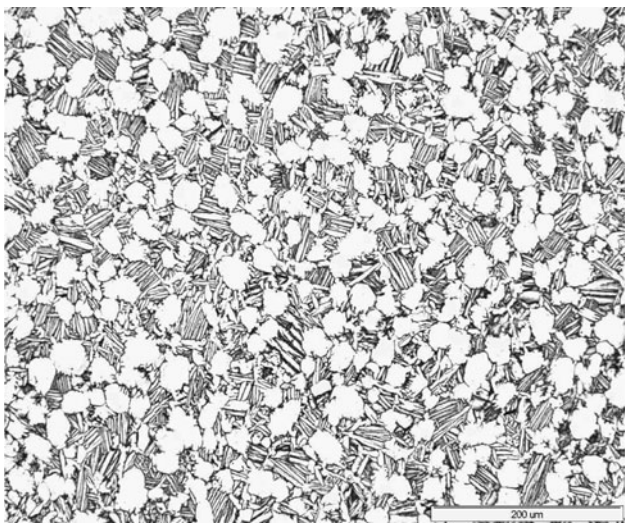

Fig. 1 Microstructure of the as-received Ti60 alloy

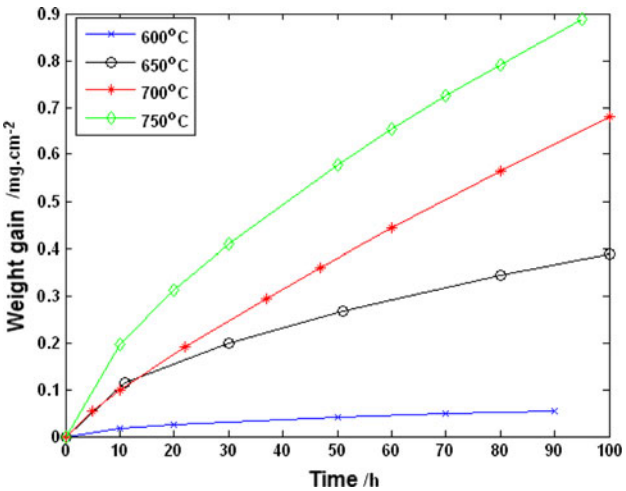

Fig. 2 The variation of weight gain with respect to oxidation time and temperature

that the oxidation rate increases sharply at the beginning of oxidation and then increases slowly.

To analyze the oxidation kinetics, the weight gain curves presented in Fig. 2 were fitted to a power type law of the form [17, 18]:

$$\Delta m^n = k_p t \quad (1)$$

where Δm is the weight gain per unit area, k_p is the rate constant, t is the oxidation time, and n is the reaction index. At a constant temperature, the kinetic model is linear if $n = 1$ and parabolic if $n = 2$.

Table 1 shows the values of the reaction index determined for the overall oxidation at the investigated temperatures. The results show that the weight gain curves obey parabolic kinetics below 700 °C. As the temperature increases to 700 °C and above, the weight gain curves tend to follow parabolic-linear kinetics, however, the parabolic kinetics is dominant during the whole tested range which can be proved by the cross-sectional morphology of the oxidized specimens shown in "Oxidation products and morphology" section.

In order to determine the activation energy of the oxidation reaction, a true parabolic kinetics was assumed over the whole temperature range. Then, Eq. 1 transforms to:

$$\Delta m^2 = k_p t \quad (2)$$

Temperature dependence of k_p can be quantified by an Arrhenius type equation [17]:

$$k_p = k_0 \exp(-Q/RT) \quad (3)$$

where k_0 is the frequency factor, Q is the activation energy, R is the gas constant (8.3143 J/(mol K)), and T is reaction temperature (K). The Q value can be calculated by plotting log k_p with respect to $1/T$. By fitting the data to the Eq. 2, the activation energy for the process of oxidation was estimated to be 256 kJ/mol. As we known, exposure of titanium alloys to any oxygen containing atmospheres at elevated temperatures leads to formation of oxide scale which including an oxide layer on the surface and alpha-case beneath it. Thus, the total weight gain represents the sum of the oxygen consumed in the formation of the surface oxide and the oxygen that diffuses into the subsurface zone. So the activation energy calculated above is the total activation energy of these two stages. The activation energy of oxidation and diffusion in selected titanium alloys are illustrated in Table 2. It may be seen that the activation energy of Ti60 alloy is quite close to the diffusion activation energy of both oxygen and titanium in TiO_2, 234 and 257 kJ/mol, respectively [19]. This suggests that the oxidation process is mainly controlled by both the outward diffusion of titanium and the inward diffusion of oxygen through the oxide scale [20]. In addition, it was also found that the activation energy of Ti60 alloy is higher than that of pure Ti and Ti-1100 alloy, and very close to that of IMI834 alloy in Ref. [21].

Table 1 Activation energy and reaction index for Ti60 alloy at 600–750 °C

Temperature (°C)	n	Q (kJ/mol)
600	1.9	256
650	1.8	
700	1.2	
750	1.5	

Oxidation products and morphology

Surface morphology of oxide scales

The surface morphologies of Ti60 alloy after oxidation in air at 600–750 °C for 100 h are shown in Fig. 3. It can be seen that the surface morphology of the specimen oxidized at 600 °C is similar to those of as-polished surface (Fig. 3a). When the oxidation temperature is 650 °C, small oxidation products are generated on the surface of specimen (Fig. 3b). At 700 °C, the oxidation products become larger than that of specimens oxidized at 650 °C, and all of the products distribute at grain boundaries of the specimens (Fig. 3c) which indicates that the oxidation products priority formation at grain boundaries during the oxidation processing. At 750 °C, surface morphologies of the specimens after oxidation are quite similar to the specimens oxidized at 700 °C. Nevertheless, some small oxides appear in the grains, as shown in Fig. 3d.

Figure 4 shows XRD patterns of Ti60 alloy oxidized at different temperatures and times. Only α-Ti peaks are detected in the specimens oxidized at 600 °C for 100 h (Fig. 4a). When oxidized at 650 and 700 °C for 100 h and 750 °C for 10 h, the peaks of TiO_2 appear (Fig. 4b–d). However, at 750 °C, the oxidation time reached to 50 and 100 h, weak diffraction signals corresponding to the Al_2O_3 phase are found (Fig. 4e, f). These results are similar with the observations obtained in other titanium alloys [14, 16, 19, 22, 23]. According to the previous report, approximately

Table 2 Activation energy of oxidation and diffusion in various titanium alloys

Material	Activation energy (kJ/mol)	Reference
Pure Ti	239	[19]
Ti-1100	225	[21]
IMI834	267	[21]
IMI834	184	[12]
O diffusion in TiO_2	234	[19]
Ti diffusion in TiO_2	257	[19]

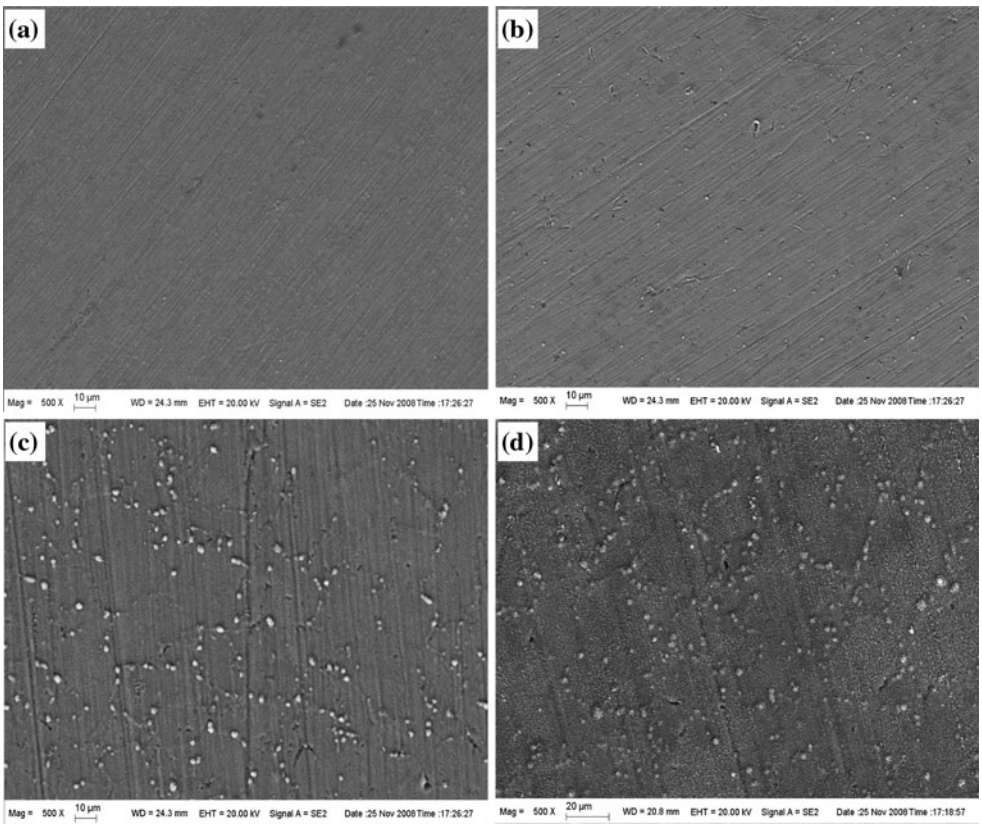

Fig. 3 The surface morphology of Ti60 alloy after 100 h oxidation in air at **a** 600 °C, **b** 650 °C, **c** 700 °C, and **d** 750 °C

57–59 at.% aluminum is needed for binary Ti–Al to form a protective alumina scale in air [24]. The aluminum contents of Ti60 alloys are well below this, thus it is not sufficient to form long lasting scale of protective and continuous alumina. Then, the oxygen ions continue to diffuse through the oxide scale. As a result, oxygen dissolution is significantly with the increase of temperature and time, which agree with the conclusion obtained from the oxidation kinetics.

Cross-sectional microstructures of oxidized specimens

Figure 5 shows the cross-sectional microstructures of Ti60 alloy oxidized at 600, 650, 700, and 750 °C for 100 h. Compared with the subsurface microstructure before oxidation, there is nearly no changes after oxidized at 600 °C (Fig. 5a). Meanwhile, the oxide scale is very thin, only about 2–5 μm. This result is in accordance with the weight gain curve of Ti60 alloy, in which the weight gain is minimal at 600 °C (Fig. 2). At 650 °C, it can be seen clearly that a white layer with thickness of about 15 μm is formed (Fig. 5b). As the temperature increases, the thickness of the layer increases to about 50 μm at 700 °C and 75 μm at 750 °C (Fig. 5c, d).

Figure 6 shows the cross-sectional microstructures of Ti60 alloy oxidized at 750 °C for 10 and 50 h. From

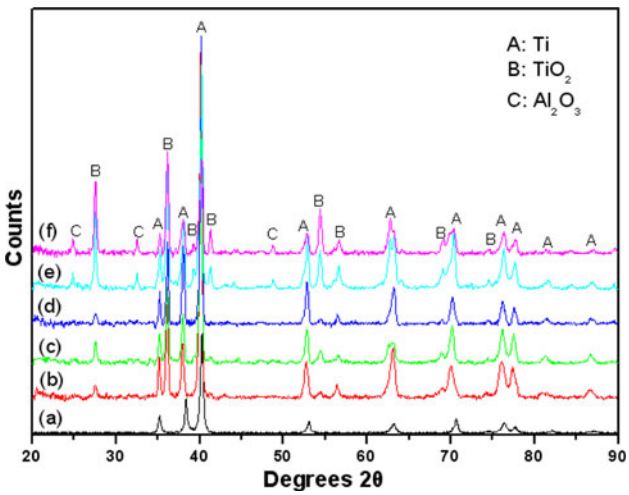

Fig. 4 XRD patterns of the specimens oxidized at (*a*) 600 °C, (*b*) 650 °C, (*c*) 700 °C for 100 h and 750 °C for (*d*) 10 h, (*e*) 50 h, (*f*) 100 h

Figs. 6 and 5d, it is clear that the thickness of the oxide scale increases with the increasing oxidation time at a constant temperature. However, the layer morphology changes with time and temperature. The surface of the oxide layer is very smooth below 700 °C, but tends to be serrate above 700 °C, especially for the specimens

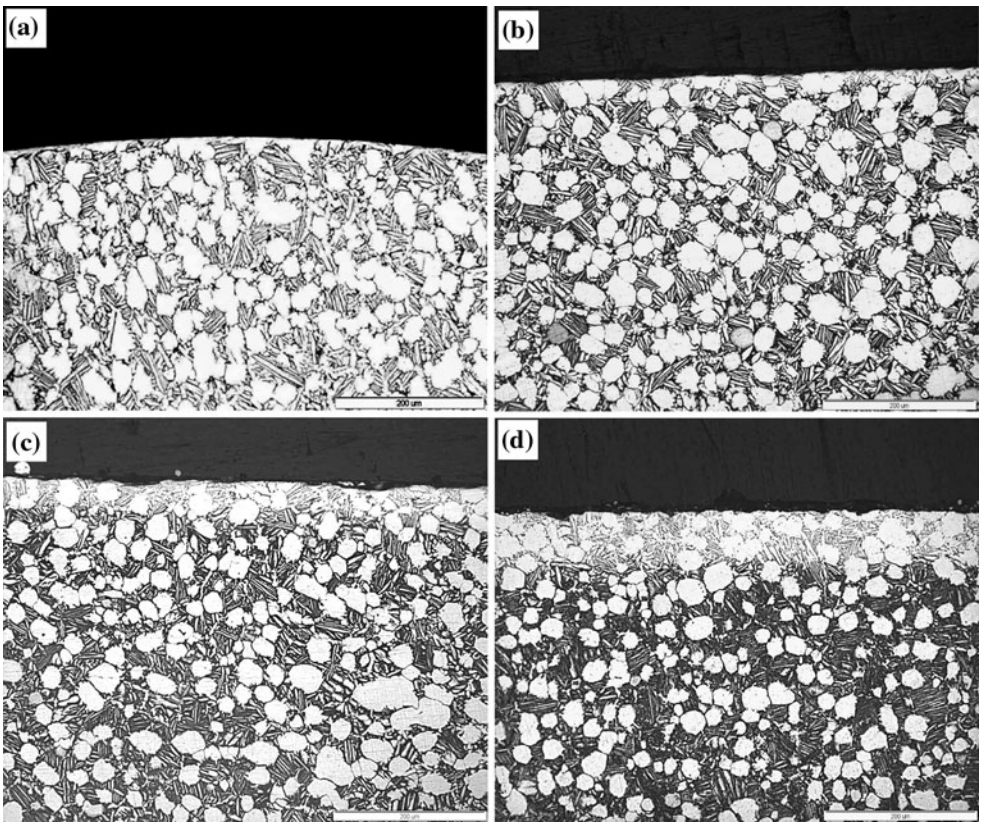

Fig. 5 Cross-sections of the scale formed after oxidized for l00 h at **a** 600 °C, **b** 650 °C, **c** 700 °C, **d** 750 °C

oxidized at 750 °C for 100 h. These phenomena indicate that the oxide layer started spalling after oxidized above 700 °C, which is in agreement with the results of Jia et al. [16]. During the oxidation temperature below 700 °C, the oxide layer was dense; it acted as a diffusion barrier that retarded the diffusion of oxygen, so the oxidation kinetics obeys the parabolic law. When the temperature above 700 °C, the oxide layer started spalling and the fresh surface was exposure which result in the oxygen diffuse rapidly. Therefore, the oxidation kinetics deviates from the parabolic law and tends to follow the linear law.

Predicting the thickness of alpha-case

In order to predict the extent of oxidation during the high temperatures, an oxidation model is proposed on the basis of several experiments at a variety of oxidation temperature and time. Due to the parabolic kinetics is dominant during

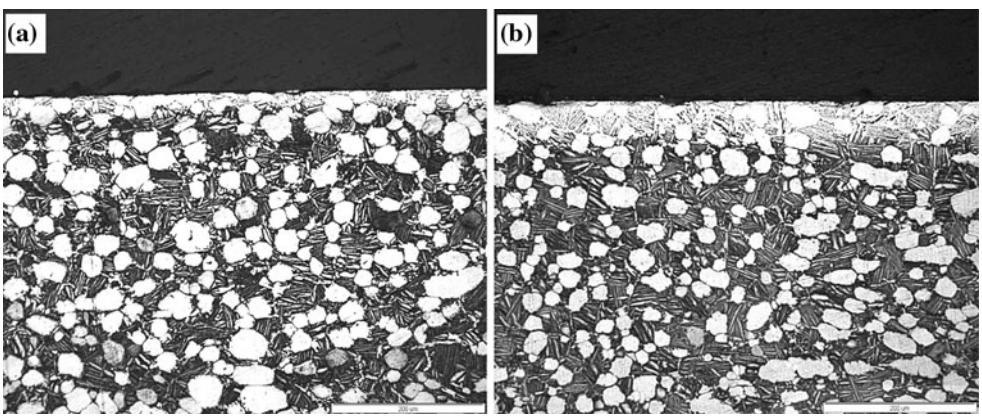

Fig. 6 Cross-sections of the scale formed after oxidized at 750 °C for **a** 10 h, **b** 50 h

the whole tested range, the diffusion distance at each temperature can be described as [22, 25]:

$$X = K(D_s t)^{1/2} \quad (4)$$

where D_s is the diffusion coefficient, X is the thickness of alpha-case (cm), K is a constant which related to the concentration of oxygen in the oxide scale, and t is the oxidation time (s). D_s can be obtained as a function of temperature:

$$D_s = D_0 \exp(-Q_s/RT) \quad (5)$$

where D_0 is the frequency factor, Q_s is the diffusion activation energy, R is the gas constant (8.3143 J/(mol K)), and T is reaction temperature (K).From Eqs. 4 and 5, the following equation can be obtained:

$$\ln\frac{X^2}{t} = \ln K^2 D_0 - \frac{Q_s}{RT} \quad (6)$$

The value of Q_s can be obtained by plotting $\ln(X^2/t)$ with respect to $1/T$. Figure 7 shows the $\ln(X^2/t)$ with $1/T$ with a good correlation coefficient of 0.97. From Fig. 7, the diffusion activation energy of 232 kJ/mol is obtained for Ti60 alloy at the whole temperature range which is close to the total activation energy of 256 kJ/mol. The result also indicates that the parabolic oxidation kinetics was dominant during the temperatures of 600–750 °C. By inserting the Q_s value and the constant into Eq. 6, the equation between X, t, and T can be obtained as follows:

$$X = [103.5t \exp(-27784/T)]^{1/2} \quad (7)$$

Equation 7 provides the predicted thickness of oxide scale as a function of oxidation time at different elevated temperatures in Ti60 titanium alloy. The predicted values are always slightly higher than the experimentally measured values. It is due to the fact that the oxidation model is proposed on the assumption that the oxidation rate controlling factor is the diffusion of oxygen through the alloy, and that the diffusion of oxygen through the growing oxide does not influence the rate of penetration.

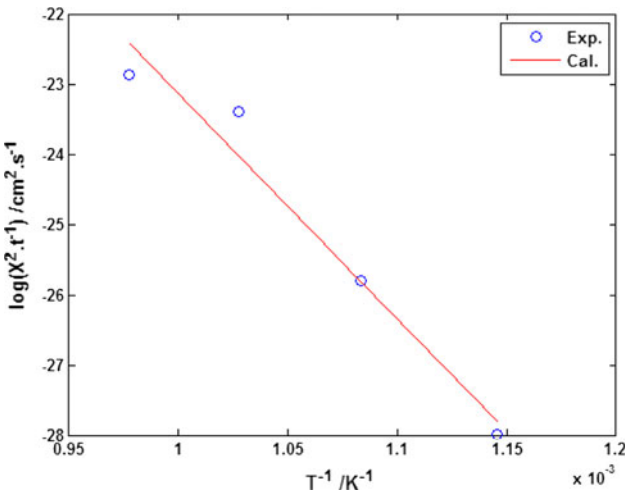

Fig. 7 The plot of $\ln(X^2/t)$ vs. $1/T$ for Ti60 specimens

Effect of oxidation on the tensile properties

In order to analyze the effect of oxidation on the tensile properties of Ti60 alloy, the specimens before and after oxidation were tested at room temperature, as shown in Fig. 8. The oxidation has a significant effect on the tensile properties of Ti60 alloy. Both of the strength and ductility decrease for the specimens with oxide scale, especially the decrease of ductility is more pronounced than that of strength. However, when the oxide scale was removed before testing, the ductility of specimens oxidized at 600 °C increases but still lower than that of initial specimens. Nevertheless, the results from the specimens oxidized at 700 and 750 °C are very interesting because they

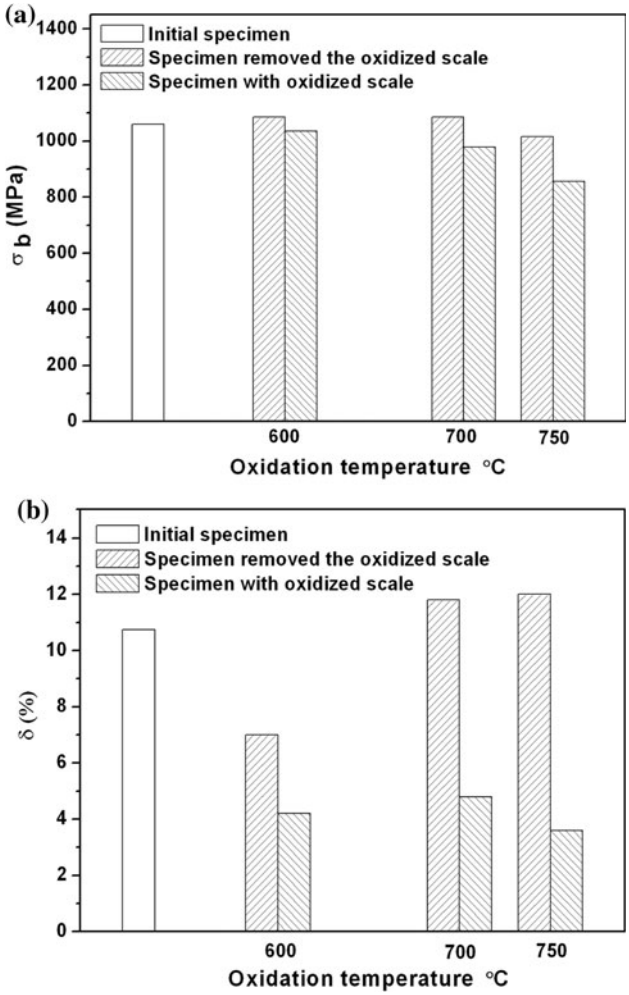

Fig. 8 Room temperature strength and elongation versus exposure temperature for Ti60 alloy

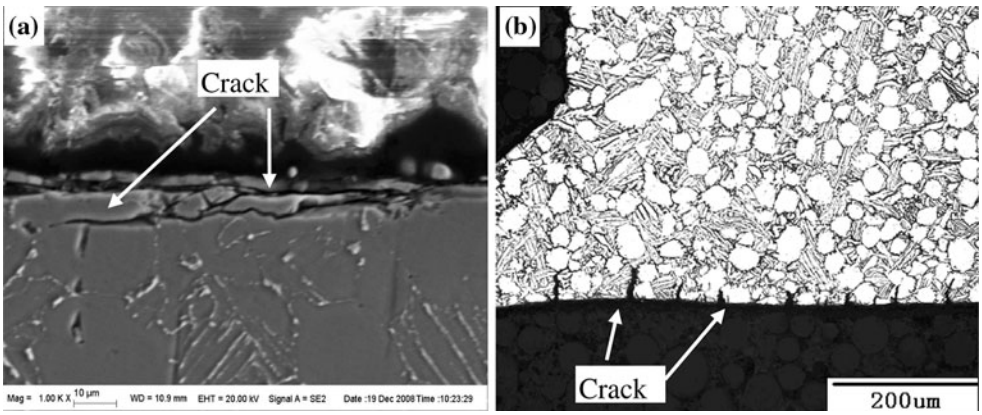

Fig. 9 Cracks in the oxidized scale of Ti60 alloy resulting from oxidation at **a** 750 °C, **b** 600 °C for 100 h

show a higher ductility compared to the initial specimens. The cause of this increase in ductility may be due to both the free of oxide scale and dissolution of α_2 particles, a similar phenomenon was observed in IMI834 and SP-700 titanium alloys [26–28]. Donlon et al. [28] also found that long-term exposure in the region of 550–600 °C can lead to a significant decrease in the ductility of β processed Ti-1100, Ti-6242S, and IMI834 alloys. All alloys exhibited a minimum in ductility of approximately 1% elongation after exposure at 600 °C. In contrast, the ductility over this temperature region in α/β IMI834 is constant in the range of 6–8%. Compared with the previous results, the thermal stability of Ti60 alloy appears to be superior to Ti-1100 and very similar to IMI834 alloy with α/β microstructure.

Several investigations have shown that the brittle alpha-case can modify the mechanical properties of titanium alloy due to the surface cracks formed. In the present study, a great number of microcracks are observed in the scale shown in Fig. 9a. Numerous publications have dealt with the formation of cracks during oxidation [17, 29, 30]. It can be concluded that two types of stresses existed in oxide during oxidation: growth stress and thermal stress. Growth stress comes from growth of the oxide on the substrate. Thermal stress results from mismatch of thermal expansion coefficients between the oxide and substrate during cooling. From Fig. 9a, it can be seen that most microcracks parallel to the oxide–metal interface, such microcracks may be developed during cooling process from oxidation temperature to room temperature. With the increasing of oxidation temperature, a thicker oxide scale formed on the surface, and many residual stress-induced cracks grew on the oxide scale during the cooling process. Under the indentation test loading, such cracks propagate into the base material (Fig. 9b), and lead to the early fracture of the samples, which results in the decrease of both ductility and strength.

Conclusions

(1) Ti60 alloy has the lowest oxidation rate at 600 °C. The weight gain curves follow parabolic kinetics below 700 °C and parabolic-linear kinetics above 700 °C, but the parabolic kinetics is dominant during the whole tested range. The total activation energy and the diffusion activation energy of oxygen in alpha-case are 256 and 232 kJ/mol, respectively.

(2) The main oxidation products were TiO_2 phase for the specimens oxidized under 700 °C for 100 h, but a mixture of TiO_2 and Al_2O_3 for the specimens oxidized at 750 °C for 50 h, and the oxidation products were preferentially formed at the grain boundaries of the alloy.

(3) With the increasing of oxidation temperature and time, the thickness of the oxide scale increases significantly and can be predicted by the equation $X = [103.5t \exp(-27784/T)]^{1/2}$.

(4) The oxidation has a significant effect on the tensile properties of Ti60 alloy. Both of the strength and ductility decrease for the specimens with oxide scale. However, both of them increase when the oxide scale was removed before testing.

Acknowledgements The authors thank the financial supports from the State Key Foundational Research Plan (Grant no. 2007CB613807) and the Program for New Century Excellent Talents in university (Grant no. NCE-07-0696).

References

1. Kearns MW, Restall JE (1988) In: Lacombe P, Tricot R, Béranger G (eds) Sixth world conference on titanium, Les Editions de Physique, Paris, p 396
2. Xiong HP, Mao W, Ma WL et al (2006) Mater Sci Eng A 433:108

3. Zhang XJ, Gao YH, Ren BY et al (2010) J Mater Sci 45:1622. doi:10.1007/s10853-009-4138-8
4. Cavalheiro AA, Bruno JC, Saeki MJ et al (2008) J Mater Sci 43:602. doi:10.1007/s10853-007-1743-2
5. Hou XM, Liu XD, Guo M et al (2008) J Mater Sci 43:6193. doi:10.1007/s10853-008-2928-z
6. Hajbagheri FA, Bozorg SFK, Amadeh AA (2008) J Mater Sci 43:5720. doi:10.1007/s10853-008-2890-9
7. Leyens C, Peters M, Kaysser WA (1997) Surf Coat Technol 94–95:34
8. Guleryuz H, Cimenoglu H (2009) J Alloys Compd 472(1–2):241
9. Lee DH, Nam SW (1999) J Mater Sci 34:2843. doi:10.1023/A:1004627216837
10. Li GP, Li D, Liu YY et al (1997) J Aeroesp Mater 17(4):21
11. Gurrappa I, Gogia AK (1999) In: Proceedings of the 5th National Convention on Corrosion, NACE International India Section, New Delhi, India
12. Nogueira RA, Grandini CR, Claro APRA (2008) J Mater Sci 43:5977. doi:10.1007/s10853-008-2706-y
13. Sai KV, Singh V (2004) Bull Mater Sci 27(4):347
14. Leyens C, Peters M, Kaysser WA (1996) Mater Sci Technol 12:213
15. Cai BC, Liu PY, Tao Y (2000) J Mater Eng 8:34
16. Jia XY, Liu PY, Tao Y (2003) J Mater Eng 6:18
17. Kofstad P (1988) High temperature corrosion. Elsevier Applied Science, Essex
18. Frangini S, Mignone A, De Riccardis F (1994) J Mater Sci 29:714. doi:10.1007/BF00445984
19. Velasco BG, Aswath PB (1998) J Mater Sci 33:2203. doi:10.1023/A:1004395908966
20. Zhang EL, Zeng G, Zeng SY (2002) Scripta Metall 46:811
21. Cui WF, Wei HR (1997) Rare Met Mater Eng 26(2):31
22. Johnson TJ, Loretto MH, Kearns MW (1993) In: Froes FH, Caplan I (eds) Titanium'92 Science and Technology, June 1992, TMS, Warrendale, San Diego, p 2035
23. Gurrappa I, Manova D, Gerlach JW et al (2006) Surf Coat Technol 201:3536
24. Meier GH, Appolonia D (1989) In: Grobstein T, Doychak J (eds) Oxidation of high temperature intermetallics. The Minerals, Metals and Materials Society, Cleveland, OH, p 185
25. Xiong HP, Mao W, Xie YH et al (2005) Mater Sci Eng A 391:10
26. Iizumi H, Fukai H (1998) In: Zhou L, Eylon D, Lutjering G, Ouchi O, (eds) Proceedings of Xi'an international titanium conference. International Academic Publishers, Beijing, China, p 526
27. Cui WF, Bian WM, Luo GZ et al (1997) J Aeroesp Mater 17(4):15
28. Donlon WT, Allison JE, Lasecki JV (1992) In: Froes FH, Caplan I (eds) Titanium'92 Science and Technology, TMS, Warrendale, San Diego, p 295
29. Garbacz H, Lewandowska M (2003) Mater Chem Phys 81(2–3):542
30. Du HL, Datta PK, Lewis DB (1996) Oxid Met 45(5/6):507